Estimating the lifetime of lanthanides on graphene for CvB-detection

Marck, Karel van der

Estimating the lifetime of lanthanides on graphene for $C\nu B-$detection

THESIS

submitted in partial fulfillment of the
requirements for the degree of

BACHELOR OF SCIENCE
in
PHYSICS

Author :	Karel van der Marck
Student ID :	s2615932
Supervisor :	Dr. Vadim Cheianov
2^{nd} corrector :	Dr. Peter Denteneer

Leiden, The Netherlands, June 24, 2022

Estimating the lifetime of lanthanides on graphene for $C\nu B-$detection

Karel van der Marck

Huygens-Kamerlingh Onnes Laboratory, Leiden University
P.O. Box 9500, 2300 RA Leiden, The Netherlands

June 24, 2022

Abstract

$\beta-$decay is associated with emitting or absorbing an electron (anti)neutrino. By measuring the energies of the other particles involved, the energy of the neutrino can be deduced and with that its mass. It is proposed to isolate an isotope in a solid-state structure, e.g. graphene or fullerene and to study the detection spectrum from $\beta-$decay inside the isotope's nucleus [E. Baracchini et al., arXiv:1808.01892]. The energy uncertainty due to the zero-point motion of the most popular isotope candidate, Tritium, has been proved to be too great for a feasible experiment [Y. Cheipesh, V. Cheianov, A. Boyarsky, Phys. Rev. D 104, 116004, (2021)]. There is, however, no theoretical objection to heavier isotopes as $\beta-$emitters in the experiment. In this thesis, the energy uncertainty (or equivalently the lifetime) of heavier isotopes due to the coupling to graphene is estimated. Also, the influence of the lifetime on the spectrum is studied.

Contents

1 Background **7**

2 Techniques **9**

3 Lifetime calculation **11**
3.1 Ground state and excited states 11
3.2 Matrix elements 12
3.3 Summing over final states 15

4 Influence of lifetime on $C\nu B-$detection **19**

5 Discussion **25**
5.1 The estimated lifetime 25
5.2 The required lifetime 27

6 Conclusion **29**

Acknowledgements **29**

Appendices **31**

A Preliminary quantum mechanics **33**
A.1 Fermi's golden rule 33
A.2 Second quantisation 36
A.3 Green's functions 39

B Anderson impurity model **43**
B.1 Different terms in Hamiltonian 43
B.2 Perturbative expansion 44
B.3 Density of states 44

Bibliography **47**

Chapter 1

Background

A.H. Becquerel discovered radioactivity in 1897 and many physicists have contributed to this discipline of study such as M.S.S. Curie and E. Rutherford. But it was not until 1930 that W.E. Pauli predicted the existence of the electron neutrino to resolve a problem with β radioactivity[1].

The problem at the time was the apparent violation of the law of energy conservation: the combined energy of the outgoing particles after $\beta-$decay should bring forth a single value, namely the energy of the ingoing particles. However, a continuous spectrum of energies was measured.

Pauli suggested the presence of an extra outgoing particle as a solution. The outgoing kinetic energy can be distributed among the different particles. Hence, the energy of the already known particles can have multiple values depending on the extent of this extra particle's kinetic energy. This explains the measured distributed spectrum. E. Fermi gave the extra particle the name *neutrino*, which is Italian for *little neutron*.

The specific neutrino in the $\beta-$decay process is the antiparticle of the electron neutrino. The reaction involved is:

$$n \rightarrow p + e + \overline{\nu}_e \tag{1.1}$$

n denotes a neutron, p a proton, e an electron and $\overline{\nu}_e$ an electron antineutrino. A similar reaction is the capture of a neutrino by a nucleus:

$$n + \nu_e \rightarrow p + e \tag{1.2}$$

Experiments from the Super-Kamiokande (SK) and the Sudbury Neutrino Observatory (SNO) provide sufficient evidence to conclude that neutrinos are not massless[2]. The mass of a neutron, proton and electron are all well-determined, but the mass of an electron neutrino is not. The PTOLEMY experiment is a pro-

posal to measure the mass of the electron neutrino by comparing the reactions 1.1 and 1.2.

The energy of the electron antineutrino from reaction 1.1 follows a distribution as discussed. At the end of this spectrum, the neutrinos have almost no kinetic energy, thus the total energy is approximately $E = m_{\overline{\nu}_e}c^2$ $(= m_{\nu_e}c^2)$. In the proposed experiment, the electron neutrino in reaction 1.2 is a relic neutrino which has almost no kinetic energy. Hence, its energy is sharply peaked around $E = m_{\nu_e}c^2$. Therefore, if both reactions occur in the same experiment, the energy difference between the broad and peaked distribution will be $\sim 2m_{\nu_e}c^2$. For this reason, the uncertainty in energy in the final products must be low enough, such that the broadening does not cause the spectra to be indistinguishable.

The initial idea was that the $\beta-$decay takes place inside a Tritium (^3H) atom enclosed in a solid-state environment. Y. Cheipesh, V. Cheianov and A. Boyarsky proved that the uncertainty in energy due to the zero-point motion of the mother isotope will be too high for a feasible experiment[3]. However, if Tritium is replaced with a heavier atom, then there is no general theoretical objection. Criteria for this atom are, among other things, the visibility of the cosmic neutrino background (CνB), the energy uncertainty due to the zero-point motion of the mother atom and the energy uncertainty of the daughter atom due to the coupling to the solid-state architecture. Taking the former two into consideration, there remain some candidates, e.g. Tm-171 and Sm-151[4]. An estimation of the latter criterion is calculated in this thesis (chapter 3).

Chapter 2 describes the ingredients we need in order to address two problems: how to find the uncertainty in energy of the β-emitter and how this affects the extent of distinguishability between the reactions 1.1 and 1.2. The basis of this approach relies on quantum mechanics and in particular the Anderson impurity model. Appendices A and B present these subjects in a nutshell. In chapter 3, the uncertainty in energy is estimated by applying Fermi's golden rule to the different states present in the Anderson impurity model. The influence on the spectra will be illustrated in chapter 4. Thereafter, the results are discussed in chapter 5 and 6.

Chapter 2

Techniques

The coupling to graphene leads to a finite lifetime of the system, i.e. the lifetime of the electronic configuration of the daughter atom is finite. The time-energy uncertainty principle tells us that a stable system* has a well-defined energy†, in other words: $\tau \Delta E \sim \hbar$. The non-zero uncertainty gives rise to a spread of the $\beta-$ and $C\nu B-$spectrum. This could lead to an overlap in the spectra, which makes it impossible to distinguish the decay types from the measured energy. Hence, the problem at hand is two-fold: we want to know the lifetime of certain solid-state designs and we want to know what the maximum allowed uncertainty is for visible $C\nu B-$detections.

We are interested in two-dimensional designs of the PTOLEMY experiment[5] and in particular Samarium or Tritium on graphene[3]. The lattice structure of graphene allows us to use the Anderson impurity model to estimate the lifetime. This model describes the energies of an impurity coupled to a lattice. We will consider the term in the Hamiltonian that described the interactions between lattice electrons and impurity electrons as a perturbation. Then, we will estimate the lifetime by Fermi's golden rule, equation A.9.

According to the Anderson impurity model, the density of states (DOS) is a Lorentzian[6]. If $\Delta E = 0$, each detection can be described by a small peak at the measured energy. Due to the coupling, we find that this is a Lorentzian instead. Since this holds for every detection, we have to convolve the ideal $\beta-$ and $C\nu B-$spectrum‡, so with $\Delta E = 0$, with a Lorentzian to find the real spectra. The ideal spectrum we will convolve is based on a calculation of $\beta-$decay in Tritium. We will plot the amount of events per year per energy on the vertical axis against the energy on the horizontal axis. Therefore, the amount of visible neutrino detections per year is the area under the non-overlapping part of the $C\nu B-$spectrum.

*With this, I mean a system with a long lifetime.

†With this, I mean the uncertainty in energy is small.

‡Both spectra are based on $\beta-$decay, but I will denote the spectrum corresponding to reaction 1.1 by β and the one corresponding to reaction 1.2 by $C\nu B$.

Chapter 3

Lifetime calculation

3.1 Ground state and excited states

According to the Anderson impurity model, a valence electron in an atom contributes to the total energy by a phenomenological parameter E_d and similarly, the presence of two electrons in the valence shell, so spin up and spin down, will contribute U to the total energy, because of the Coulomb repulsion between the electrons. In other words, $\hat{H}_{impurity}|00\rangle = 0$, $\hat{H}_{impurity}|10\rangle = E_d|10\rangle$, $\hat{H}_{impurity}|01\rangle = E_d|01\rangle$ and $\hat{H}_{impurity}|11\rangle = (2E_d + U)|11\rangle$ where $\hat{H}_{impurity} = \sum_\sigma E_d \hat{n}_{d\sigma} + U\hat{n}_{d\uparrow}\hat{n}_{d\downarrow}$ and where the first ket component represents the occupation of a spin up electron and the second spin down.

The ground state of impurity is the lowest energy state. The lowest energy state depends on the values of the E_d and U. If $E_d = 0$ and $U > 0$, one can see that $|00\rangle$, $|10\rangle$, $|01\rangle$ are all ground states. Hence, the line $E_d = 0$ is a boundary between two ground state regimes as long as $U > 0$. The same logic applies for the boundaries $2E_d + U = 0$ and $E_d = 2E_d + U$. A visualisation of the three ground state regions with the corresponding boundary plots is given in figure 3.1.

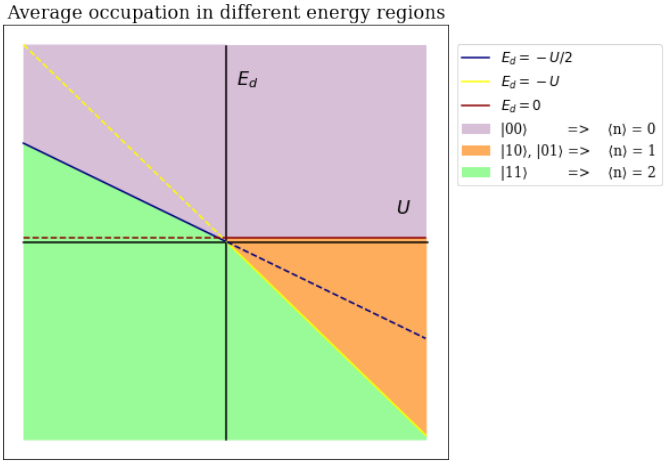

Figure 3.1: *The ground state of the system depends on the values E_d and U. The line, $E_d = 0$, is plotted slightly above the $U-$axis merely for visual purposes, but in a faithful diagram they should coincide. The dashed lines are not boundaries between ground state regions, but the analytical continuation of such boundaries.*

When coupling the impurity to the lattice, in our case graphene, electrons may be shared between the impurity and the lattice. Therefore, the ground state is a linear combination of the quantised charge states. A corresponding ground state diagram would not have strict boundaries, but rather a continuum of ground states which are superpositions of the former ground states. In this case, we get a broadening in the DOS.

Fermi's golden rule may be applied to calculate the lifetime of the system. The coupling is the perturbation that might excite the initial state. However, the initial state (projected on the Hilbert space of the impurity) is not the mother atom (before the $\beta-$decay), nor the daughter atom. It is the daughter atom with the electronic configuration of the mother atom.

Samarium coupled to graphene on Ir(111); Sm@GR/Ir(111), has a net charge transfer of 0.83 ± 0.03 based on density functional theory (DFT) calculations[7]. We will approximate the charge transfer to be 1 so that we can approximate the DOS with a delta function. The validity of this assumption is discussed in chapter 5. Sm-151 has an even number of electrons, so after the charge transfer an odd number of electrons. Therefore, the ground state of the impurity will be $|10\rangle$ or $|01\rangle$. Let us assume $|01\rangle$.

3.2 Matrix elements

The interaction Hamiltonian in the Anderson impurity model is given by $\hat{H}' = \sum_{\sigma k} V_k \hat{c}^\dagger_{\sigma k} \hat{d}_\sigma$. This is explained in appendix B. We will modify this to a local description: instead of summing over k in reciprocal space, we integrate over positions x in real space. For this, we need to use field operators $\hat{\psi}_{\sigma g}(x)$, $\hat{\psi}^\dagger_{\sigma g}(x)$, $\hat{\psi}_{\sigma d}(x)$, $\hat{\psi}^\dagger_{\sigma d}(x)$ for the graphene electrons and impurity electrons respectively instead of the creation/annihilation operators $\hat{c}_{\sigma k}$, $\hat{c}^\dagger_{\sigma k}$, $\hat{d}_\sigma$, $\hat{d}^\dagger_\sigma$.

The problem at hand is two-dimensional, so the field operators have the dimension of inverse length: $\hat{\psi}(x) \propto \frac{1}{\sqrt{A}}$ with A the area in real space. The interaction part becomes $\hat{H}' = \sum_\sigma \int d^2x \; V(x) \hat{\psi}^\dagger_{\sigma g}(x) \hat{\psi}_{\sigma d}(x) + H.C.$

We look at the effect of only one impurity*, so naturally the wavefunction of the impurity has a position dependence. Therefore, we write $\hat{\psi}_{\sigma d} = \frac{\hat{d}_\sigma}{\sqrt{A}}$ where $\hat{d}_\sigma$ is an annihilation operator in the impurity. The interaction term simplifies to $\hat{H}' = \frac{1}{\sqrt{A}} \sum_\sigma \int d^2x \; V(x) \hat{\psi}^\dagger_{\sigma g} \hat{d}_\sigma + H.C.$

We define the following Fourier transformations.

$$\begin{cases} V(x) = \int \frac{d^2x}{2\pi} \, e^{i\vec{k}\cdot\vec{x}} \, V_k \\ V_k = \int \frac{d^2x}{2\pi} \, e^{-i\vec{k}\cdot\vec{x}} \, V(x) \end{cases} \qquad \begin{cases} \hat{\psi}_{\sigma g}(x) = \int \frac{d^2x}{2\pi} \, e^{i\vec{k}\cdot\vec{x}} \, \hat{\psi}_{\sigma k} \\ \hat{\psi}_{\sigma k} = \int \frac{d^2x}{2\pi} \, e^{-i\vec{k}\cdot\vec{x}} \, \hat{\psi}_{\sigma g}(x) \end{cases}$$

*An impurity has only a small effect on electrons far away. There may be more impurities, but if they are distributed with a large enough average distance from one another, then the electrons would feel the effect of maximally one impurity.

Version of June 24, 2022– Created June 24, 2022 - 13:49

These Fourier transformations may be conjugated to get the transformations of $V(x)^*$, V_k^*, $\hat{\psi}^\dagger_{g\sigma}(x)$ and $\hat{\psi}^\dagger_{k\sigma}$. Subsequently, we get

$$\begin{aligned}\hat{H}' &= \frac{1}{\sqrt{A}}\sum_\sigma \int d^2x \, \frac{\int d^2k \int d^2k'}{(2\pi)^2} \, e^{+i\vec{k}\cdot\vec{x}} e^{-i\vec{k}'\cdot\vec{x}} \, V_{k'} \, \hat{\psi}^\dagger_{\sigma k}\hat{d}_\sigma + H.C. \\ &= \frac{1}{\sqrt{A}}\sum_\sigma \frac{\int d^2k \int d^2k'}{(2\pi)^2} \, (2\pi)^2\delta(\vec{k}-\vec{k}') \, V_{k'} \, \hat{\psi}^\dagger_{\sigma k}\hat{d}_\sigma + H.C. \\ &= \frac{1}{\sqrt{A}}\int d^2k \sum_\sigma V_k \, \hat{\psi}^\dagger_{\sigma k}\hat{d}_\sigma + H.C.\end{aligned}$$

It is noteworthy that this V_k is not the same as the V_k used in the regular Anderson impurity model. Here, $V_k \propto A$, because it is a Fourier transformed quantity and V_k in the Anderson impurity model is independent of the area.

Thus far, we have implicitly assumed the graphene lattice to be a squared grid. This is the reason we could integrate over $x-$space and $k-$space in the continuum limit. However, the actual structure is a honeycomb lattice. This means that the symmetry group is C_3 viewed from a site, but D_6 viewed from a cell. The first view gives rise to a way of generating half of the space with two lattice vectors[8].

A neighbouring pair of carbon atoms can therefore span the whole lattice. This gives rise to a new quantum number, α, called the valley. The valley remains present in the Fourier domain: each unit cell contains six points at which the conduction band and valence band meet, three of those correspond to $\alpha = -1$ and three to $\alpha = +1$. In the proximity of these points, the dispersion relation is linear, so around the meeting points there are so-called *Dirac cones*. The linear relation is given in equation 3.1.

$$\epsilon_k = \alpha|k|\hbar v_F \tag{3.1}$$

Here v_F is the Fermi velocity in graphene, which is approximately 10^6 ms^{-1}. For our purposes, we use the relation $\epsilon_k = \alpha|k|\hbar v_F - \mu$ where μ is the chemical potential, since we deal with a many-body system.

The Fourier transformed field operator $\hat{\psi}_{\sigma k}$ is called an *eigenmode* of graphene and has been calculated in terms of creation and annihilation operators[8]. This is presented in equation 3.2.

$$\hat{\psi}_{\sigma k} = \sqrt{\frac{A}{2}}\sum_\alpha \left[\hat{c}_{\sigma k\alpha}u_{k\alpha} + \hat{c}^\dagger_{\sigma k\alpha}v_{(-k)\alpha}\right] \tag{3.2}$$

The terms u and v are some normalised two-component vectors. The *spinor* 3.2 is a solution to the Dirac equation with eigenenergy 3.1. We will use equation 3.2 to substitute in the expression of $\hat{H}'$ and equation 3.1 in calculating the matrix elements of the perturbation between the initial state and final states.

We have assumed that the initial state of the impurity is $|01\rangle$, thus the initial state of our system must be $|i\rangle = |01\rangle \otimes |FS\rangle$ where $|FS\rangle$ is the ground state of the

graphene or in other words, the *Fermi sea* (FS). We write $|i\rangle = |vac\rangle$. Two types of transitions described by the Anderson impurity model are the emittance of an impurity electron to the graphene and the emittance of a graphene electron to the impurity[†]. Therefore, the final states are

$$\begin{cases} |f^{(1)}_{k\alpha}\rangle = \hat{d}^\dagger_\uparrow \hat{c}_{\uparrow k\alpha}\,|vac\rangle \\ |f^{(2)}_{k\alpha}\rangle = \hat{d}_\downarrow \hat{c}^\dagger_{\downarrow k\alpha}\,|vac\rangle \end{cases} \tag{3.3}$$

These final states are allowed for different k and α. After we have constructed the matrix elements, we will sum over the different possibilities in Fermi's golden rule (section 3.3). The first matrix element becomes

$$\begin{aligned} \langle i|\hat{H}'|f^{(1)}_{k\alpha}\rangle &= \langle vac|\Big(\frac{1}{\sqrt{A}}\int d^2k' \sum_\sigma V_{k'}\, \hat{d}^\dagger_\sigma \hat{\psi}_{\sigma k'} + H.C.\Big)\hat{d}^\dagger_\uparrow \hat{c}_{\uparrow k\alpha}|vac\rangle \\ &= \langle vac|\Big(\frac{1}{\sqrt{A}}\int d^2k' \sum_\sigma V_{k'}\, \hat{d}^\dagger_\sigma \Big[\sqrt{\frac{A}{2}}\sum_{\alpha'}\big[\hat{c}_{\sigma k'\alpha'}u_{k'\alpha'} \\ &\quad + \hat{c}^\dagger_{\sigma k'\alpha'}v_{(-k')\alpha'}\big]\Big] + H.C.\Big)\hat{d}^\dagger_\uparrow \hat{c}_{\uparrow k\alpha}\,|vac\rangle \end{aligned} \tag{3.4}$$

Due to the commutation relations of $\hat{d}$, we find that only the $H.C.$ part of this equation will remain.

$$\begin{aligned} \langle i|\hat{H}'|f^{(1)}_{k\alpha}\rangle &= \langle vac|\Big(\frac{1}{\sqrt{A}}\int d^2k' \sum_\sigma V^*_{k'}\, \hat{d}_\sigma \Big[\sqrt{\frac{A}{2}}\sum_{\alpha'}\big[\hat{c}^\dagger_{\sigma k'\alpha'}u^*_{k'\alpha'} \\ &\quad + \hat{c}_{\sigma k'\alpha'}v^*_{(-k')\alpha'}\big]\Big]\Big)\hat{d}^\dagger_\uparrow \hat{c}_{\uparrow k\alpha}\,|vac\rangle \\ &= \sqrt{\frac{A}{2}}\frac{1}{\sqrt{A}}\int d^2k' \sum_{\sigma\alpha'} V^*_{k'}\ \langle vac|\Big(\hat{d}_\sigma\big[\hat{c}^\dagger_{\sigma k'\alpha'}u^*_{k'\alpha'} \\ &\quad + \hat{c}_{\sigma k'\alpha'}v^*_{(-k')\alpha'}\big]\Big)\hat{d}^\dagger_\uparrow \hat{c}_{\uparrow k\alpha}\,|vac\rangle \\ &= \frac{1}{\sqrt{2}}\int d^2k'\ V^*_{k'}\ u^*_{k'\alpha}\ \langle 01|\hat{d}_\uparrow \hat{d}^\dagger_\uparrow|01\rangle \cdot \langle FS|\hat{c}^\dagger_{\uparrow k'\alpha}\hat{c}_{\uparrow k\alpha}|FS\rangle \\ &= \frac{1}{\sqrt{2}}A^{-1}\ V^*_k\ u^*_{k\alpha}\theta(\mu - \epsilon_{\uparrow k\alpha}) \end{aligned} \tag{3.5}$$

The last equation holds, since $\langle vac|\hat{c}^\dagger_{\uparrow k'\alpha}\hat{c}_{\uparrow k\alpha}|vac\rangle = (2\pi)^2 A^{-1}\delta(k-k')\theta(\mu - \epsilon_{k\alpha})$. Since the spinor $u_{k\alpha}$ is normalised, we conclude that the squared matrix element will be

$$|\,\langle i|\hat{H}'|f^{(1)}_{k\alpha}\rangle\,|^2 = \frac{|V_k|^2}{2A^2}\,\theta(\mu - \epsilon_{\uparrow k\alpha}) \tag{3.6}$$

[†]There are more possible processes, e.g. Auger processes, but the omittance thereof will be discussed in chapter 5.

Version of June 24, 2022– Created June 24, 2022 - 13:49

Similarly, one can verify that the square of the second matrix element is

$$| \langle i|\hat{H'}|f^{(2)}_{k\alpha}\rangle |^2 = \frac{|V_k|^2}{2A^2}\,\theta(\epsilon_{\downarrow k\alpha} - \mu) \tag{3.7}$$

3.3 Summing over final states

The uncertainty in energy of the final products can be estimated using Fermi's golden rule and the Heisenberg uncertainty principle, $\Delta E\tau \sim \hbar$ where τ the lifetime of the system. Namely, $\Delta E \sim \frac{\hbar}{\tau} = \hbar\Gamma_{i\to f}$ and by Fermi's golden rule $\Gamma_{i\to f} = \frac{2\pi}{\hbar}\sum_f | \langle i|\hat{H'}|f\rangle |^2\rho(E_i - E_f)$. This is derived in appendix A.

In section 3.1 we mentioned an approximation of the DOS by delta functions. This gives us a way to simplify our expression: the sum may be transformed to an integral in the continuum limit and integrating over a delta function is equivalent to the evaluation of the integrand.

$$\begin{aligned}\Delta E &= 2\pi\sum_f | \langle i|\hat{H'}|f\rangle |^2\delta(E_i - E_f)\\ &= 2\pi\sum_{k\alpha}\frac{|V_k|^2}{2A^2}\big(\theta(\mu - \epsilon_{\uparrow k\alpha})\delta(E_i - E^{(1)}_{k\alpha}) + \theta(\epsilon_{\downarrow k\alpha} - \mu)\delta(E_i - E^{(2)}_{k\alpha})\big)\end{aligned} \tag{3.8}$$

The summation of final states has been specified to a summation of k, α and the matrix elements have been substituted in equation 3.8. The terms $E^{(1)}_{k\alpha}$, $E^{(2)}_{k\alpha}$ represent the energy of state $|f^{(1)}_{k\alpha}\rangle$, $|f^{(1)}_{k\alpha}\rangle$ respectively. The initial energy is $E_i = (E_d - \mu) + \sum_{k'\alpha'\in FS}(\epsilon_{k'\alpha'} - \mu)$ and the final energies are

$$\begin{cases} E^{(1)}_{k\alpha} = 2(E_d - \mu) + U - (\epsilon_{k\alpha} - \mu) + \sum_{k'\alpha'\in FS}(\epsilon_{k'\alpha'} - \mu)\\ E^{(2)}_{k\alpha} = (\epsilon_{k\alpha} - \mu) + \sum_{k'\alpha'\in FS}(\epsilon_{k'\alpha'} - \mu)\end{cases}$$

The sum over $k'\alpha' \in FS$ denotes the sum over the different electrons in the Fermi sea. By subtraction, it follows that

$$\begin{cases} E_i - E^{(1)}_{k\alpha} = \epsilon_{k\alpha} - (E_d + U)\\ E_i - E^{(2)}_{k\alpha} = E_d - \epsilon_{k\alpha}\end{cases}$$

We will plug these values into the delta functions in order to calculate the uncertainty in energy. Then, we will use the dispersion relation in graphene to change the coordinates to $k-$space. Since we assumed the ground state to be $|01\rangle$, we have constraints on E_d and U which will limit the amount of delta functions that may contribute to the uncertainty. We will further assume that the function V_k does not depend substantially on the specific value of k, so there is a V such that $\forall k : V \simeq V_k$.

Version of June 24, 2022– Created June 24, 2022 - 13:49

$$
\begin{aligned}
\Delta E &= 2\pi \sum_{k\alpha} \frac{|V_k|^2}{2A^2} \big(\theta(\mu - \epsilon_{\uparrow k\alpha})\delta(\epsilon_{k\alpha} - (E_d + U)) + \theta(\epsilon_{\downarrow k\alpha} - \mu)\delta(E_d - \epsilon_{k\alpha})\big) \\
&= \frac{\pi}{A^2} \sum_{k\alpha} |V_k|^2 \big(\theta(\mu - \epsilon_{\uparrow k\alpha})\delta(\alpha\hbar v_F|k| - \mu - (E_d + U)) \\
&\quad + \theta(\epsilon_{\downarrow k\alpha} - \mu)\delta(E_d - (\alpha\hbar v_F|k| - \mu))\big) \\
&= \frac{\pi}{A^2} \sum_{k\alpha} |V_k|^2 \big(\theta(\mu - \epsilon_{\uparrow k\alpha}) \frac{1}{\hbar v_F} \delta(|k| - \frac{\alpha}{\hbar v_F}(E_d + U + \mu)) \\
&\quad + \theta(\epsilon_{\downarrow k\alpha} - \mu) \frac{1}{\hbar v_F} \delta(|k| - \frac{\alpha}{\hbar v_F}(E_d + \mu))\big) \\
&= \frac{\pi}{A^2} \sum_{k} |V_k|^2 \big(\theta(\mu - \epsilon_{\uparrow k(+1)}) \frac{1}{\hbar v_F} \delta(|k| - \frac{1}{\hbar v_F}(E_d + U + \mu)) \\
&\quad + \theta(\epsilon_{\downarrow k(-1)} - \mu) \frac{1}{\hbar v_F} \delta(|k| + \frac{1}{\hbar v_F}(E_d + \mu))\big) \\
&\simeq \frac{\pi |V|^2}{A^2 \hbar v_F} \sum_{k} \big(\theta(\mu - \epsilon_{\uparrow k(+1)})\delta(|k| - \frac{1}{\hbar v_F}(E_d + U + \mu)) \\
&\quad + \theta(\epsilon_{\downarrow k(-1)} - \mu)\delta(|k| + \frac{1}{\hbar v_F}(E_d + \mu))\big)
\end{aligned}
\tag{3.9}
$$

Let us substitute the so-called hybridisation energy, $V_H = \frac{V}{A}$. This quantity is independent of the real space area A just as the uncertainty in energy. However, if we transform the sum into an integral, $\sum_k \to \frac{A}{(2\pi)^2} \int d^2k = \frac{A}{2\pi} \int k dk$, we get an area dependence. This is permitted, because we integrate over the reciprocal space and the bigger the area gets, the smaller the values of the differential d^2k.

However, we integrate over delta functions, so this compensating effect disappears. The compensating effect must therefore be transferred to the hybridisation energy. In other words, a large area corresponds to a small hybridisation energy. Then, the uncertainty will have no functional dependence of the area. Thus, the area could only slightly affect the value of ΔE, but this originates solely from the extent to which the continuum limit applies.

$$
\begin{aligned}
\Delta E &= \frac{\pi |V_H|^2}{\hbar v_F} \frac{A}{2\pi} \int dk \big(k\theta(\mu - \epsilon_{\uparrow k(+1)})\delta(|k| - \frac{1}{\hbar v_F}(E_d + U + \mu)) \\
&\quad + k\theta(\epsilon_{\downarrow k(-1)} - \mu)\delta(|k| + \frac{1}{\hbar v_F}(E_d + \mu))\big) \\
&= \frac{|V_H|^2 A}{2\hbar v_F} \int dk \big(k\theta(\mu - \epsilon_{\uparrow k(+1)})\delta(|k| - \frac{1}{\hbar v_F}(E_d + U + \mu)) \\
&\quad + k\theta(\epsilon_{\downarrow k(-1)} - \mu)\delta(|k| + \frac{1}{\hbar v_F}(E_d + \mu))\big) \\
&= \frac{|V_H|^2 A}{2(\hbar v_F)^2} \big((E_d + U + \mu)\theta(\mu - (E_d + U)) - (E_d + \mu)\theta(E_d - \mu)\big)
\end{aligned}
\tag{3.10}
$$

Version of June 24, 2022– Created June 24, 2022 - 13:49

The hybridisation energy of Sm@GR is $\sim 0.1\ eV$ with a corresponding area of $(10\ \text{Å})^2$ based on density functional theory calculations (DFT)[9].

We can translate these Heaviside step functions into three different regimes: $\mu < E_d$, $E_d < \mu < E_d + U$ and $E_d + U < \mu$. It is noteworthy that the chemical potential may be tuned‡. Thus, if one is capable of tuning μ to be greater than E_d and less than $E_d + U$, then the uncertainty in energy can be reduced significantly. Namely,

$$\begin{aligned}
\Delta E &= \frac{|V_H|^2 A}{2(\hbar v_F)^2} \begin{cases} -E_d - \mu & \mu < E_d \\ 0 & E_d < \mu < E_d + U \\ E_d + U + \mu & E_d + U < \mu \end{cases} \\
&\simeq \frac{(0.1\ eV \cdot 10\ \text{Å})^2}{2(10^{-34} Js \cdot 10^6 \frac{m}{s})^2} \begin{cases} -E_d - \mu & \mu < E_d \\ 0 & E_d < \mu < E_d + U \\ E_d + U + \mu & E_d + U < \mu \end{cases} \\
&\simeq 10^{-2} \cdot \begin{cases} -E_d - \mu & \mu < E_d \\ 0 & E_d < \mu < E_d + U \\ E_d + U + \mu & E_d + U < \mu \end{cases}
\end{aligned} \tag{3.11}$$

If $\mu < E_d$, then it is energetically favourable for the impurity to donate an electron and if $\mu > E_d + U$ it is energetically favourable to receive an electron. At these energies, the system is not in a ground state, thus there will be a finite lifetime which is implies an uncertainty in energy. This can be seen directly from equation 3.11. If $E_d < \mu < E_d + U$, then the system is in a ground state and an infinite lifetime implies certainty of the energy. One should bear in mind that there are other types of physical events that can play a role in the energy uncertainty, e.g. Auger processes. These will be relatively dominant in the case where $E_d < \mu < E_d + U$.

If the values of E_d, U and μ are of the order $\sim 1\ eV$, then $\Delta E \sim 10^{-2}\ eV \ll 2m_{\nu_e} \simeq 0.24\ eV$. Here, the upper bound of the sum of neutrino masses, $\sum m_\nu$, is taken[10]. However, that is only the uncertainty of one detection. The combination of the uncertainty in all the measurements will cause the two spectra to spread out over more energies. As mentioned in chapter 1, the end of the $\beta-$spectrum will come closer to the tail of the $C\nu B-$spectrum and vice versa. The distinguishability will be investigated in chapter 4.

The uncertainty $\Delta E \sim 10^{-2}\ eV$ corresponds to a lifetime of $\tau \sim 10^{-13}\ s$ by the energy-time uncertainty principle.

‡This can be done by coupling the graphene to another material, for example another layer of graphene. We are, however, somewhat limited, since $E_d, U \gg V_H$. If this inequality is not satisfied, perturbation theory breaks down and so does our estimation of ΔE.

Version of June 24, 2022– Created June 24, 2022 - 13:49

Chapter 4

Influence of lifetime on $C\nu B-$detection

In this chapter we will estimate the allowed* energy uncertainty of Tritium atoms due to the electronic coupling to graphene. The *classical* spectra are based conservation laws regarding reactions 1.1 and 1.2[3]. With *classical*, I mean that our calculation of ΔE is not incorporated.

The horizontal axis of figure 4.1 represents the energy of the outgoing electron with a translation such that the domain of the $\beta-$spectrum contains negative energies and the domain of the $C\nu B-$spectrum positive energies, in other words, we describe the rest frame of the Tritium atom. The vertical axis represents the detection rate per energy.

The points in the $\beta-$spectrum range from $-10\,eV$ to $0\,eV$, but we want to include the effect of lower energies as well. The points follow a quadratic curve from energies close to the origin down to multiple keV below zero†. This also holds for the $\beta-$spectra of Thulium and Samarium. We apply a least squares method to extend the domain of the Tritium $\beta-$spectrum. Additionally, the detection rate per energy is extended to positive energies with an array of zeros. A visual representation is given in figure 4.1.

*With allowed, I mean that the $C\nu B-$spectrum can be distinguished from the $\beta-$spectrum.

†This is based on data from the IAEA:
https://www-nds.iaea.org/relnsd/vcharthtml/VChartHTML.html.

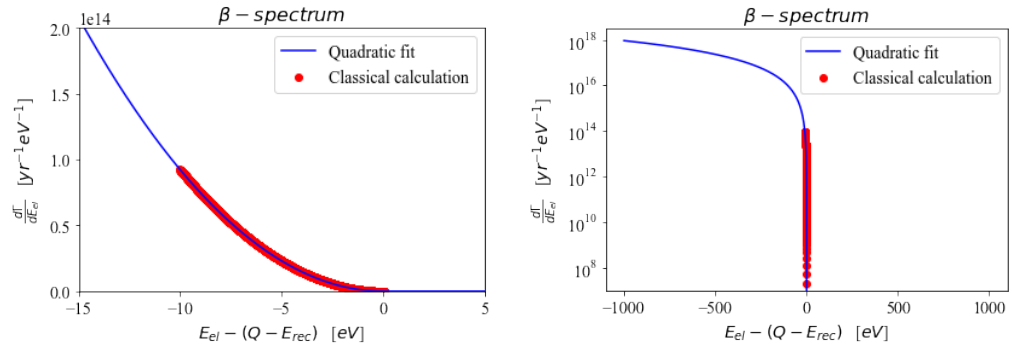

(a) *The quadratic fit of the (calculated) data from* $-15\ eV$ *to* $5\ eV$.

(b) *The quadratic fit on a log scaled plot. The energies range from* $-1000\ eV$ *to* $1000\ eV$.

Figure 4.1: *The linearly and logarithmically scaled plot of the quadratic fit.*

From appendix B, we know that the density of states is a Lorentz distribution ($\mathcal{L}$). To adjust for the whole spectrum (β), we apply a convolution, equation 4.1.

$$\beta_{corrected}(E) = (\beta_{classical} \star \mathcal{L})(E) := \int_{-\infty}^{+\infty} d\tilde{E}\ \ \beta_{classical}(\tilde{E})\mathcal{L}(E - \tilde{E}) \tag{4.1}$$

We are particularly interested in energies E near the neutrino energy. We will assume that the $C\nu B-$spectrum is centered around $0.05\ eV$. This assumption will be discussed in chapter 5. We will distinguish a low energy and a high energy regime from one another in this integral. The lowest energy of the $\beta-$spectrum is roughly $-18\ keV$.

$$(\beta \star \mathcal{L})(E) = \int_{-18\ keV}^{-1\ keV} d\tilde{E}\ \ \beta(\tilde{E})\mathcal{L}(E - \tilde{E}) + \int_{-1\ keV}^{0} d\tilde{E}\ \ \beta(\tilde{E})\mathcal{L}(E - \tilde{E}) \tag{4.2}$$

We will assume that the $\beta-$spectrum is still "reasonably well-described" by the quadratic fit $\beta(x) = Ax^2 + Bx + C$ down to some energy of the low energy regime, so $(-18\ keV, -1\ keV)$, and that the other energies will not contribute substantially to the convolution. We will elaborate on this in chapter 5. Let us assume this energy is roughly $-15\ keV$. We will show that the low energy term in the convolution will be independent of the energy E, which is chosen near the neutrino energy. For this, we will use that for all $\tilde{E} < -1\ keV$: $A\tilde{E}^2 + B\tilde{E} + C \approx A\tilde{E}^2$ and $\frac{\Delta E}{\tilde{E}^2 + (\Delta E)^2} \approx \frac{\Delta E}{\tilde{E}^2}$.

$$\begin{aligned}\int_{-18\ keV}^{-1\ keV} d\tilde{E}\ \ \beta(\tilde{E})\mathcal{L}(E-\tilde{E}) &\approx \int_{-18\ keV}^{-1\ keV} d\tilde{E}\ \ \beta(\tilde{E})\mathcal{L}(-\tilde{E}) \\ &\approx \int_{-15\ keV}^{-1\ keV} d\tilde{E}\ \ (A\tilde{E}^2+B\tilde{E}+C)\frac{\Delta E}{(-\tilde{E})^2+(\Delta E)^2} \\ &\approx \int_{-15\ keV}^{-1\ keV} d\tilde{E}\ \ A\tilde{E}^2\frac{\Delta E}{\tilde{E}^2} \\ &= 16\ keV\cdot A\Delta E \\ &\approx 10^{15}\ eV^{-2}yr^{-1}\cdot\Delta E\end{aligned} \tag{4.3}$$

The last equality follows from the value of the fit parameter $A \sim 10^{11}\ eV^{-3}yr^{-1}$. From now on, we will consider only the high energy term, $\int_{-1\ keV}^{0} d\tilde{E}\ \ \beta(\tilde{E})\mathcal{L}(E-\tilde{E})$, in the numerical analysis and we will adjust the end result with the additional factor of the low energy term if necessary.

Not only the $\beta-$spectrum, but also the $C\nu B-$spectrum is prone to the uncertainty in energy, so we convolute both with a Lorentz distribution. The uncertainty in energy is related to the width of the Lorentzian. This changes the spread in the distribution as can be seen in figure 4.2. In the figure, low uncertainties correspond to the graphs with dark colours. One can see that the $C\nu B-$spectra with low uncertainties converge to the original spectrum. The convergence to the original $\beta-$spectrum is slower: for positive energies, the values of $\frac{d\Gamma}{dE_{el}}$ should fall down to zero.

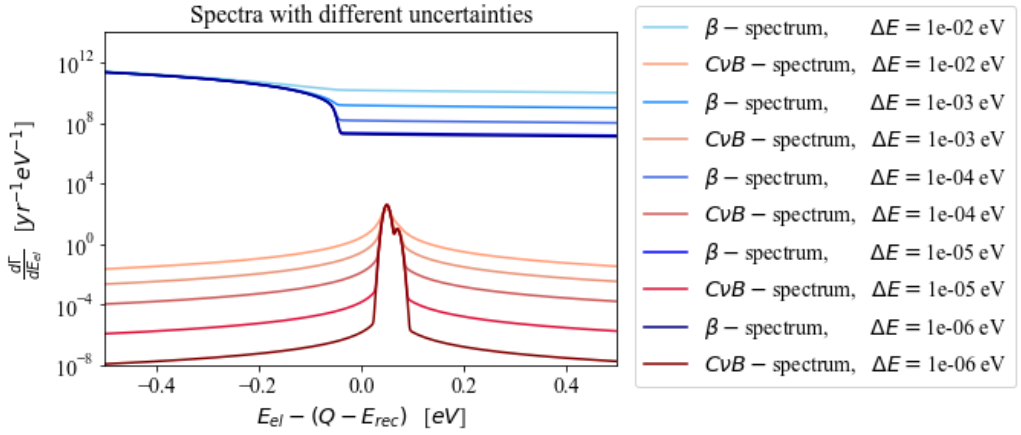

Figure 4.2: *The uncertainty in energy broadens the distributions.*

Note that the graphs of $\Delta E = 10^{-5}\ eV$ and $\Delta E = 10^{-6}\ eV$ of the $\beta-$spectrum coincide. This is a numerical effect and arises from a discrete convolution instead of a continuous one. For the calculated data, this effect would arise at $\Delta E =$

$10^{-3}\ eV$, but in figure 4.2, there are 100 times as many points taken into account by the employment of linear interpolation.

Another noteworthy phenomenon is the apparent increase of the area below the $C\nu B-$spectrum that occurs when increasing ΔE. This originates from the logarithmically scaled vertical axis and the large amount of displayed detection rates per energy. In figure 4.3, one can see that the height of the $C\nu B-$spectrum descends, therefore the area remains the same.

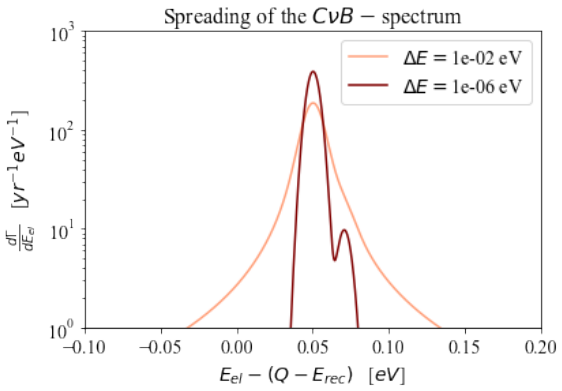

Figure 4.3: *A plot of the broadening of the $C\nu B-$spectrum.*

By focussing on the $\beta-$spectrum in figure 4.2, one notices that decreasing the uncertainty in energy by an order of magnitude, the event rate per energy is approximately decreased by the same order of magnitude. This is more clearly illustrated in figure 4.4.

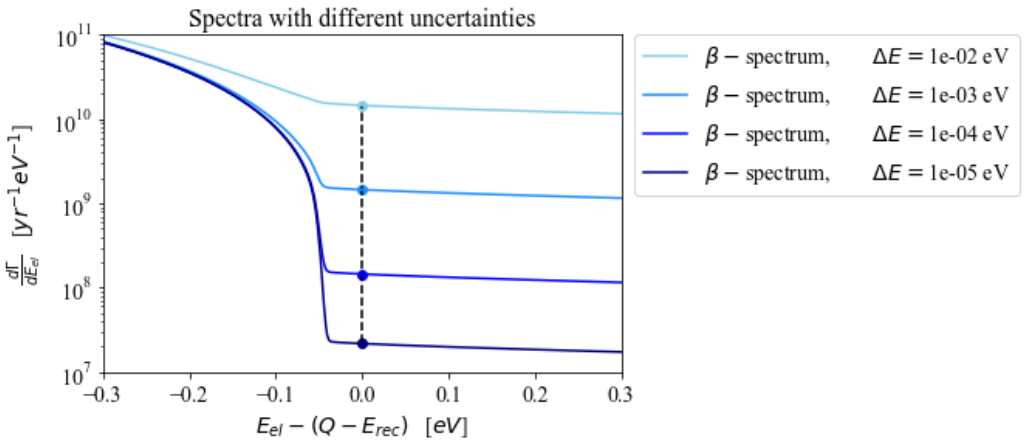

Figure 4.4: *A reduction of uncertainty in energy leads to a lower detection rate per energy for positive energies.*

One can verify this linear relationship by performing the analytical convolution. The considered uncertainties are less than or equal to $10^{-2}\ eV \ll E$ where E is an energy near the neutrino mass. Then,

Version of June 24, 2022– Created June 24, 2022 - 13:49

$$
\begin{aligned}
(\beta \star \mathcal{L})(E) &= \int_{-\infty}^{+\infty} d\tilde{E}\ \ \beta(\tilde{E})\mathcal{L}(E-\tilde{E}) \\
&\approx \int_{-\infty}^{0} d\tilde{E}\ \ \beta(\tilde{E})\mathcal{L}(-\tilde{E}) \\
&= \int_{-\infty}^{0} d\tilde{E}\ \ \beta(\tilde{E})\frac{\Delta E}{(-\tilde{E})^2+(\Delta E)^2} \\
&\approx \int_{-\infty}^{0} d\tilde{E}\ \ \beta(\tilde{E})\frac{\Delta E}{(-\tilde{E})^2} \\
&\propto \Delta E
\end{aligned}
\tag{4.4}
$$

The peak of the $C\nu B-$spectrum is roughly $4 \cdot 10^2\ yr^{-1}eV^{-1}$, but an uncertainty of $\Delta E \sim 10^{-2}\ eV$ produces a $\beta-$spectrum of $\sim 10^{10}\ eV^{-1}yr^{-1}$ at the same energy. This means, that if we would extrapolate the behaviour in figure 4.4, then the we need to have $\Delta E < 10^{-10}\ eV$ to obtain a nonzero detection rate.

However, from figure 4.4 we can see that $\frac{d\Gamma}{dE_{el}} \approx 10^{12}\ eV^{-2}yr^{-1} \cdot \Delta E$. Thus, the additional term from the low energy regime is significant, which is $10^{15}\ eV^{-2}yr^{-1} \cdot \Delta E$. Therefore, we need to have $\Delta E < 10^{-13}\ eV$ to have a nonzero detection rate. This corresponds to a lifetime of $\tau > 10^{-2}\ s$.

Version of June 24, 2022– Created June 24, 2022 - 13:49

Chapter 5

Discussion

5.1 The estimated lifetime

In this thesis, the uncertainty in energy of the final products of a Samarium atom after $\beta-$decay due to the coupling to graphene is estimated. It is calculated that a single detection of an electron's energy would yield an uncertainty in the order of $10^{-2}\ eV$. Underlying to this result a series of assumptions have been employed. For example, we have assumed that the initial state of the impurity is $|01\rangle$. A different choice would result in different processes, so the regimes of equation 3.11 would change, but the order of magnitude does not.

Another assumption is the employment of the continuum limit. The sum over final states transforms to an integral by assuming an infinite area. The area from the DFT calculation to compute the hybridisation energy is a grid of 32 unit cells[9]. By the inverse square law of the electric field, the electrons far away from the impurity feel little coupling, therefore, one can argue that the continuum limit is justified in the case of 32 unit cells. However, this limit implies a squared lattice, while graphene has a honeycomb lattice.

Furthermore, we approximated that the hybridisation energy, V_H, is independent of the quasi-momentum k. This is a conventional approximation - it is also utilised for the DFT calculation (of Sm@GR) that brought forth the value of V_H that we have adopted[9]. In addition, the charge transfer from Samarium to graphene on Ir(111), ΔQ, is based on DFT[7]. The latter result might differ from a calculation on Sm@GR instead of Sm@GR/Ir(111). Needless to say, experiments, e.g. *photoemission spectroscopy* (PES) and for our purposes specifically the ultraviolet case (UPS), would be more reliable.

The determined value of ΔQ for Sm@GR/Ir(111) is 0.83 ± 0.03, which is not an integer. This broadens the DOS, but we neglected this effect and substituted $\rho(E_i - E_f) = \delta(E_i - E_f)$. This simplified the integral of equation 3.11. We obtained a value of ΔE and performed the convolution (chapter 4) of the 'classical'

$\beta-$spectrum with a Lorentzian with the obtained ΔE. We note that, in this calculation, the Lorentzian behaviour is not omitted.

The values of the hybridisation energy and charge transfer in the lifetime calculation are based on Samarium as the impurity. This is simply based on the available literature. However, other rare-earth elements (lanthanides) have chemical similarities - they are $f-$block elements* - so the method of calculating the lifetime would not differ substantially. Moreover, a rough estimate suffices, so we are merely interested in knowing the order of magnitude of the lifetime.

The energies of graphene electrons become apparent when the system falls down to the ground state from an excited state, so e.g. an electron is transferred from the impurity to the graphene. Then, by the conservation law of energy, the electron will retain its energy in graphene. This is typically a low energy ($\sim eV$), therefore the linear dispersion approximation of equation 3.1 is valid.

According to equation 3.11, the energy uncertainty of a single detection depends considerably on the value of μ - the uncertainty may even be reduced to zero. This is not physical: the assumption was that the coupling is the most substantial perturbation, but if the initial state is the ground state, other processes become relatively more important.

The Auger effect is an example thereof: an $s-$shell electron is emitted and a valence electron falls down to the $s-$shell. As seen in appendix B, the Anderson impurity model has equivalent diagrams to the Hartree approximation. Therefore, we have omitted all diagrams except for the hybridisation and interaction term. The inclusion of these processes in the analysis is beyond the scope of this thesis.

Tuning the chemical potential such that the daughter atom after $\beta-$decay is stable in the solid-state environment would be the most efficient way to reduce tunnelling processes, but it is not investigated how to do this in this thesis. We have described an alternative, namely to reduce direct tunnelling. Another experimental technique would be to attach the decaying atom onto an insulator to reduce all tunnelling processes, i.e. direct and indirect processes.

We note that the found uncertainty in energy has a quadratic dependence on the hybridisation energy. Thus, if e.g. the DFT value is one order of magnitude smaller or greater than the experimental value, then the uncertainty will be off by two orders of magnitude.

*Except for Lutetium.

5.2 The required lifetime

An ideal numerical analysis of the problem at hand would include all the energies of the $\beta-$spectrum and the convolution integration variable dE would be small enough such that the Lorentzians with small ΔE are well-defined on the domain. Such a computation is beyond the scope of this thesis. Instead we have exploited some analytical properties of the $\beta-$spectrum, we extrapolated the function to low energies and we estimated a sufficient lifetime for a visible $C\nu B-$spectrum.

For example, we have assumed that the $\beta-$spectrum can be approximated with a quadratic polynomial from $-15\ keV$ to $0\ eV$. This may be an imprecise approximation, but we are merely interested in obtaining the right order of magnitude of ΔE. The choice of $-15\ keV$ is based on the detection rate at lower energies: this is lower than the detection rate at $-15\ keV$, hence we can further assume that these energies will not substantially affect the convolution near the neutrino energy.

Furthermore, we have interpolated the calculated $\beta-$spectrum with 100 points between two calculated values. This way, the energy steps are small enough so that narrow Lorentzians can be distinguished from one another. In figure 4.2 the Lorentzians with $\Delta E = 10^{-5}\ eV$ and $\Delta E = 10^{-6}\ eV$ are indistinguishable because of too little interpolation, while they should differ by an order of magnitude.

The latter follows from figure 4.4. The reason as to why the event rate per energy is linearly proportional to the uncertainty in energy is that $\mathcal{L}(E - \tilde{E}) \propto \Delta E$ as explained in equation 4.4. This verifies our extrapolation to the convolution with even narrower Lorentzians without numerically simulating this.

Figure 4.4 also shows that the exact choice of m_{ν_e} for the $C\nu B-$spectrum will not massively influence the final result of the required lifetime, since the $\beta-$spectrum is a slightly descending plateau for positive energies. The lifetime corresponds to the height of this plateau and a small change in the center of the $C\nu B-$spectrum will not determine whether the spectrum will rise above the plateau or not.[†]

Ultimately, we are interested in the spectra of $\beta-$decay in lanthanides, but we have investigated only Tritium. Based on data of the IAEA, we conclude that the $\beta-$spectra of Thulium and Samarium are also approximated well by quadratic polynomials. Therefore, a similar analysis is appropriate. However, the intensity of the $\beta-$ and $C\nu B-$spectra can be different for these lanthanides and accordingly the signal-to-noise ratio[‡].

[†]However, one can argue that a logarithmically plotted descending plateau is actually polynomially decreasing, but we will disregard this argument, since a choice of the center of the $C\nu B-$spectrum is of the $meV-$scale.

[‡]Here, we regard the $\beta-$spectrum as noise.

Version of June 24, 2022– Created June 24, 2022 - 13:49

Chapter 6

Conclusion

We have seen that by tuning the chemical potential of the graphene, the uncertainty in energy due to direct tunnelling might vanish completely. However, we have not studied the consequences of indirect tunnelling processes or possibilities to avert any uncertainty in energy, so this requires further investigation.

We have seen that the tails of Lorentz distributions add up to great heights when performing convolutions. This makes $C\nu B-$detection rather difficult: by studying the spectra of Tritium we found that the required lifetime for visible events must be higher than $10^{-2}\ s$. This corresponds to a lower energy uncertainty than $10^{-13}\ eV$ that originates from the coupling to graphene. We will leave the analysis of these requirements for Thulium and Samarium for future studies.

Acknowledgements

I would like to thank Mr. V. Cheianov and Ms. Y. Cheipesh for their supervision and teaching during my bachelor project. I have learned a lot from the many pleasant interactions we have had. Furthermore, I am grateful to Mr. V. Cheianov and Mr. P. Denteneer for being the first and second reader of this thesis. Also, I would like to thank Mr. A. Boyarsky for his teaching.

Appendices

Appendix A

Preliminary quantum mechanics

A.1 Fermi's golden rule

A.1.1 Time-dependent perturbation theory

Suppose we have a two-level system, so an unperturbed quantum system with two orthogonal state solutions: $\hat{H}^0\psi_i = E_i\psi_i$; $\langle\psi_i|\psi_j\rangle = \delta_{ij}$; $i, j \in \{a, b\}$. Then, the state is described by a linear combination of the two levels evolving in time.

$$\Psi(t) = c_a(t)\psi_a e^{-i\frac{E_a}{\hbar}t} + c_b(t)\psi_b e^{-i\frac{E_b}{\hbar}t} \tag{A.1}$$

The functions c_a, c_b encode the probability that one finds the system in state a, b respectively. The normalisation of Ψ is governed by these functions. The exclusion of exponential time factors $e^{i\frac{E_a}{\hbar}t}$, $e^{-i\frac{E_a}{\hbar}t}$ in $c_a(t)$, $c_b(t)$ is arbitrary.

Let us now perturb the system with Hamiltonian $\hat{H}'$. Applying the Schrödinger equation to equation A.1, one finds that

$$c_a(t)\big(\hat{H}'\psi_a\big)e^{-i\frac{E_a t}{\hbar}} + c_b(t)\big(\hat{H}'\psi_b\big)e^{-i\frac{E_b t}{\hbar}} = i\hbar\big(\dot{c}_a(t)\psi_a e^{-i\frac{E_a}{\hbar}t} + \dot{c}_b(t)\psi_b e^{-i\frac{E_b}{\hbar}t}\big) \tag{A.2}$$

Since ψ_a and ψ_b are orthogonal, we can simplify equation A.2 by taking the inner product with ψ_a. For simplicity, we will assume that $H_{aa} = H_{bb} = 0$ where $H_{ij} = \langle\psi_i|\hat{H}'|\psi_j\rangle$. This results in a partial differential equation (PDE), equation A.3.

$$\begin{cases} \dot{c}_a(t) = -\frac{i}{\hbar}H'_{ab}e^{-i\omega_0 t}c_b(t) \\ \dot{c}_b(t) = -\frac{i}{\hbar}H'_{ba}e^{i\omega_0 t}c_a(t) \end{cases} \tag{A.3}$$

Here, $\omega_0 := \frac{E_b - E_a}{\hbar}$. Our perturbation, $\hat{H}'$, can have various forms. Let us assume that it is constant. However, the final formula, Fermi's golden rule, will also hold for sinusoidal perturbations for example*. A first order approximation

*For this, it is important that the driving frequency of the perturbation is close to ω_0.

Version of June 24, 2022– Created June 24, 2022 - 13:49

will suffice, so we do not need to solve the PDE. If the system starts in state a ($c_a(0) = 1$), then our so-called 'zeroth order' approximation tells us that $\hat{H}' \approx 0$, so the system stays in state a. The first order approximation uses equation A.3: the zeroth order values may be inserted on the right hand side and then we integrate over the left hand side. This is shown in equation A.4.

$$\begin{cases} c_a(t) = 1 \\ c_b(t) = -\frac{i}{\hbar}\int_0^t dt'\ H'_{ba}e^{i\omega_0 t'} \end{cases} \tag{A.4}$$

Note that the normalisation is satisfied to the first order in $\hat{H}'$: $|c_a(t)|^2 + |c_b(t)|^2 = 1 + \mathcal{O}(\hat{H}')$. The integral is fairly straightforward, equation A.5.

$$\begin{aligned} c_b(t) &= -\frac{i}{\hbar}\int_0^t dt'\ H'_{ba}e^{i\omega_0 t'} = -\frac{i}{\hbar}H'_{ba}\int_0^t dt'\ e^{i\omega_0 t'} = -\frac{H'_{ba}}{\hbar\omega_0}(e^{i\omega_0 t} - 1) \\ &= -\frac{H'_{ba}}{\hbar\omega_0}e^{i\frac{\omega_0}{2}t}(e^{i\frac{\omega_0}{2}t} - e^{-i\frac{\omega_0}{2}t}) = -\frac{2iH'_{ba}}{\hbar\omega_0}e^{i\frac{\omega_0}{2}t}sin(\frac{\omega_0}{2}t) \end{aligned} \tag{A.5}$$

The probability to find the system in state b is

$$P_b = |c_b(t)|^2 = \frac{|H'_{ba}|^2}{\hbar^2\omega_0^2}\cdot 4sin^2(\frac{\omega_0}{2}t) = \frac{|H'_{ab}|^2}{\hbar^2}\cdot\frac{sin^2(\frac{\omega_0}{2}t)}{(\frac{\omega_0}{2})^2} \tag{A.6}$$

However, we have thusfar only described the transition from one bound state (a) to another (b). Often, the perturbation excites a particle from a bound state to a *bath* of final states, also known as *scattering states*. This means that we do not have only one excited state, E_b, but a region around it as well, $E_b \pm \delta E$. We can adjust the probability found in equation A.6 by integrating the expression times the density of states (DOS) over this energy region. We will assume that the DOS will vary slowly with the scattering energies.

$$\begin{aligned} P_b &= \int_{E_b-\delta E}^{E_b+\delta E} d\tilde{E}_b\ \frac{|H'_{ab}|^2}{\hbar^2}\cdot\frac{sin^2(\frac{\tilde{\omega}_0}{2}t)}{(\frac{\tilde{\omega}_0}{2})^2}\rho(\tilde{E}_b) \\ &= \frac{|H'_{ab}|^2}{\hbar^2}\rho(E_b)\int_{E_b-\delta E}^{E_b+\delta E} d\tilde{E}_b\ \frac{sin^2(\frac{\tilde{\omega}_0}{2}t)}{(\frac{\tilde{\omega}_0}{2})^2} \end{aligned} \tag{A.7}$$

A substantial part of the area below a $sinc^2$ function is in the first few oscillations. Therefore, we will set the integration bounds of A.7 to $\pm\infty$. Then, we can use a standard integral, $\int_{\mathbb{R}} dx sinc^2(x) = \pi$. If we set $x = \frac{\tilde{\omega}_0 t}{2}$, then $dx = \frac{t}{2\hbar}d\tilde{E}_b$. We obtain the decay probability, equation A.8.

$$P_b = \frac{2\pi}{\hbar}|H'_{ab}|^2\rho(E_b)t \tag{A.8}$$

We will change our notation as follows: $a \to i$, $b \to f$, $H'_{ab} \to \langle i|\hat{H}'|f\rangle$, $P_b \to P_{i\to f}$. The decay rate is given by the derivative of the decay probability. Fermi's golden rule follows, equation A.9.

Version of June 24, 2022– Created June 24, 2022 - 13:49

$$\Gamma_{i\to f} = \frac{P_{i\to f}}{dt} = \frac{2\pi}{\hbar} |\langle i|\hat{H}'|f\rangle|^2 \rho(E_f) \tag{A.9}$$

A.1.2 Relation to Heisenberg uncertainty principle

By the energy-time uncertainty principle, $\tau\Delta E \sim \hbar$, where τ is the lifetime of a system and ΔE the uncertainty in energy.[†] This means that systems with long lifetimes have a well-defined energy and systems with short lifetimes do not.

Per definition, $\Gamma_{i\to f} = \frac{1}{\tau}$, so $\Delta E \sim \frac{\hbar}{\tau} = \hbar\Gamma_{i\to f} = 2\pi|\langle i|\hat{H}'|f\rangle|^2\rho(E_f)$. This means that, if a perturbation $\hat{H}'$ causes a system to decay from state $|i\rangle$ to state $|f\rangle$, then there is some intrinsic uncertainty in energy of the final products. It is noteworthy that the energy of the final products does not necessarily equal the energy of the initial particles. In other words, the total energy is not conserved.

Suppose a perturbed system has a long lifetime, thus perturbation theory is still applicable at times $t \gg \frac{1}{\omega_0}$. Since $\frac{1}{\pi}\lim_{n\to\infty}\frac{sin^2(nx)}{nx^2} = \delta(x)$, equation A.7 becomes

$$\begin{aligned}
P_b &= \frac{|H_{ab}|^2}{\hbar^2}\int_{E_b-\delta E}^{E_b+\delta E} d\tilde{E}_b\; t\cdot\left(\pi\delta(\frac{\tilde{\omega}_0}{2})\right)\cdot\rho(\tilde{E}_b) \\
&= \frac{\pi}{\hbar^2}|H_{ab}|^2 t\int_{E_b-\delta E}^{E_b+\delta E} d\tilde{E}_b\;\delta(\frac{\tilde{E}_b - E_a}{2\hbar})\rho(\tilde{E}_b) \\
&= \frac{2\pi}{\hbar}|H_{ab}|^2 t\int_{E_b-\delta E}^{E_b+\delta E} d\tilde{E}_b\;\delta(\tilde{E}_b - E_a)\rho(\tilde{E}_b) \\
&= \frac{2\pi}{\hbar}|H_{ab}|^2 t\rho(E_a) \\
\Gamma_b &= \frac{2\pi}{\hbar}|H_{ab}|^2\rho(E_a)
\end{aligned} \tag{A.10}$$

Comparing this equation with Fermi's golden rule, one can see that energy is conserved, which is expected for systems with long lifetimes.

[†]More generally, if Δt is the time it takes for the expectation value of an observable to change with one standard deviation and ΔE the uncertainty in energy, then $\Delta t\Delta E \geq \frac{\hbar}{2}$.

Version of June 24, 2022– Created June 24, 2022 - 13:49

A.2 Second quantisation

A significant part of this section is based on the book *'Condensed Matter Field Theory'* by A. Altland and B.D. Simons[11].

A.2.1 Occupation number representation

Quantum mechanics has revolutionised the theory of microscopic particles, but the consequences are not limited to small systems. Suppose we have N identical particles. The wavefunction can be constructed by (anti-)symmetrisation arguments of fermions and bosons respectively. The combined wave function lives in the sum of the individual Hilbert spaces, $\mathcal{H}^N$, and can be written as

$$|\lambda_1 \dots \lambda_N\rangle = \frac{1}{\sqrt{N! \sum_{\lambda=0}^{\infty}(n_\lambda!)}} \sum_{\mathcal{P}} \zeta^{\frac{1-sgn\mathcal{P}}{2}} |\lambda_{\mathcal{P}(1)}\rangle \otimes \cdots \otimes |\lambda_{\mathcal{P}(N)}\rangle \tag{A.11}$$

Here, we sum over permutations $\mathcal{P}$ and we have defined the number ζ as $+1$ for bosons and -1 for fermions. The normalisation constant contains factors n_λ which denote the occupation number of state λ. Although the representation in equation A.11 is correct, one would have to perform a gigantic number of calculations for macroscopic systems ($N \sim \mathcal{O}(10^{23})$). Especially since inner products between two states would require $(N!)^2$ inner products between single particle states.

We transform to the so-called *occupation number representation*. Instead of writing the kets in terms of the single particle states λ_i, we write it in terms of the number of times a particle occupies such a state, so $|\lambda_1 \dots \lambda_N\rangle \to |n_1 n_2 \dots\rangle$, where n_i denotes the occupation number of λ_i. This representation is less redundant: one does not have to write multiple times whether one single particle state is occupied.

We write the space of occupation states $|n_1 n_2 \dots\rangle$ as $\mathcal{F}^N$, where $\sum_i n_i = N$. Similar to the grand canonical ensemble, we can even remove the fixed particle condition. A large enough space to contain all the states is $\mathcal{F} = \bigoplus_{N=0}^{\infty} \mathcal{F}^N$. This is called the *Fock space*. We notice that $\mathcal{F}^0$ is included - this is a one-dimensional Hilbert space that contains a *vacuum state*, $|0\rangle$, not to confuse with 0[‡].

[‡]The vacuum has properties, i.e. operators may have nonzero eigenvalues when acting on vacuum. An example is a quantum harmonic oscillator where the vacuum has energy.

Version of June 24, 2022– Created June 24, 2022 - 13:49

A.2.2 Creation and annihilation operators

We are interested in creating all states of the Fock space with a constructive method. For this purpose we introduce the linear operators $\hat{a}_i^\dagger : \mathcal{F} \to \mathcal{F}$ called *creation operators*. They are defined by

$$\hat{a}_i^\dagger \left|n_1 \dots n_i \dots\right\rangle := \zeta^{s_i} \sqrt{n_i + 1} \left|n_1 \dots n_i + 1 \dots\right\rangle \tag{A.12}$$

where $s_i = \sum_{j=1}^{i-1} n_j$. Relation A.13 is then satisfied.

$$\left|n_1 n_2 \dots\right\rangle = \prod_i \frac{1}{\sqrt{n_i!}} (a_i^\dagger)^{n_i} \left|0\right\rangle \tag{A.13}$$

This is the reason why the operators, $\hat{a}_i^\dagger$, are called creation operators. By taking the conjugate of equation A.12, we can construct the so-called *annihilation operators*, $\hat{a}_i$, which are the hermitian adjoint of $\hat{a}_i^\dagger$. These are

$$\hat{a}_i \left|n_1 \dots n_i \dots\right\rangle = \zeta^{s_i} \sqrt{n_i} \left|n_1 \dots n_i - 1 \dots\right\rangle \tag{A.14}$$

With these properties, we can derive the occupation number operator, equation A.15.

$$\begin{aligned} \hat{a}_i^\dagger \hat{a}_i \left|n_1 \dots n_i \dots\right\rangle &= \hat{a}_i^\dagger \zeta^{s_i} \sqrt{n_i} \left|n_1 \dots n_i - 1 \dots\right\rangle \\ &= \zeta^{s_i} \sqrt{n_i} \hat{a}_i^\dagger \left|n_1 \dots n_i - 1 \dots\right\rangle \\ &= \zeta^{s_i} \sqrt{n_i} \zeta^{s_i} \sqrt{(n_i - 1) + 1} \left|n_1 \dots n_i \dots\right\rangle \therefore \hat{n}_i = \hat{a}_i^\dagger \hat{a}_i \\ &= \zeta^{2s_i} n_i \left|n_1 \dots n_i \dots\right\rangle \\ &= n_i \left|n_1 \dots n_i \dots\right\rangle \end{aligned} \tag{A.15}$$

$\therefore \hat{n}_i = \hat{a}_i^\dagger \hat{a}_i$

From equations A.12 and A.14, different commutation relations can be obtained, equation A.16.

$$\begin{cases} [\hat{a}_i, \hat{a}_j]_\zeta = [\hat{a}_i^\dagger, \hat{a}_j^\dagger]_\zeta = 0 \\ [\hat{a}_i, \hat{a}_j^\dagger]_\zeta = \delta_{ij} \end{cases} \tag{A.16}$$

Here, the commutator $[.,.]_\zeta$ is defined as $[\hat{A}, \hat{B}]_\zeta := \hat{A}\hat{B} - \zeta \hat{B}\hat{A}$.

Version of June 24, 2022– Created June 24, 2022 - 13:49

A.2.3 One-body and two-body operators

So far we have managed to construct the Fock space out of creation operators and we have exploited the properties of the creation and annihilation operators. Now, we want to express all observables in terms of these operators. Often, this is a straightforward calculation, since we have an occupation number operator. For example, a free Hamiltonian may be expressed as the sum of all single particle Hamiltonians. So, $\hat{H}\left|\psi\right\rangle = \sum_n \hat{H}_n \left|\psi\right\rangle = \sum_n d_n E_n \left|\psi\right\rangle$ where d_n is the degeneracy of the n'th energy. This is naturally equivalent to the expectation value of the occupation number, therefore, $\hat{H}\left|\psi\right\rangle = \sum_n \left\langle\hat{n}\right\rangle E_n \left|\psi\right\rangle = \sum_n E_n \left\langle\hat{n}\right\rangle \left|\psi\right\rangle = \sum_n E_n \hat{n} \left|\psi\right\rangle$, thus $\hat{H} = \sum_n E_n \hat{n}$.

We have only considered discrete quantum states and energy levels so far, but the continuum case is quite similar. Our $\hat{a}_i^\dagger$, $\hat{a}_i$ transform to $\hat{a}^\dagger(\vec{r})$, $\hat{a}(\vec{r})$ and the Kronecker delta function in the commutation relation A.16 becomes a Dirac delta function. Now, the formalism does not revolve around the occupation number, but the local density: $\hat{a}^\dagger(\vec{r})\hat{a}(\vec{r}) = \rho(\vec{r})$. The free Hamiltonian becomes $\hat{H} = \int d^d r \;\; \hat{a}^\dagger(\vec{r}) \left[\frac{\vec{p}^2}{2m} + V(\vec{r})\right] \hat{a}(\vec{r})$. This is a *one-body operator*, i.e. there is only one local density present, so we are describing either the energy of only one particle or of multiple non-interacting particles.

To describe interactions, we need *two-body operators*. Namely, if we have a system of N interacting particles with the Coulomb interaction $V(\vec{r}, \vec{r'})$, then we can write the interaction operator as

$$\hat{V}\left|\vec{r}_1 \ldots \vec{r}_N\right\rangle = \sum_{n<m}^{N} V(\vec{r}_n, \vec{r}_m) \left|\vec{r}_1 \ldots \vec{r}_N\right\rangle \tag{A.17}$$

This is simply a summation of all individual interaction energies. We can write this as a sum over all n and to prevent double counting we multiply by $\frac{1}{2}$, equation A.18.

$$\hat{V}\left|\vec{r}_1 \ldots \vec{r}_N\right\rangle = \frac{1}{2}\sum_{n=1}^{N} V(\vec{r}_n, \vec{r}_m) \left|\vec{r}_1 \ldots \vec{r}_N\right\rangle \tag{A.18}$$

By the same reasoning as earlier, we can translate our expression to the continuum case. This is given in equation A.19.

$$\hat{V}\left|\vec{r}_1 \ldots \vec{r}_N\right\rangle = \frac{1}{2}\int d^d r \int d^d r' \;\; \hat{a}^\dagger(\vec{r})\hat{a}^\dagger(\vec{r'})V(\vec{r}, \vec{r'})\hat{a}(\vec{r})\hat{a}(\vec{r'}) \tag{A.19}$$

Version of June 24, 2022– Created June 24, 2022 - 13:49

A.3 Green's functions

A significant part of this section is based on the book *'A Guide to Feynman Diagrams in the Many-Body Problem'* by R.D. Mattuck[12].

A.3.1 Solving differential equations

Suppose we have a linear differential operator $\mathcal{D}$ such that for functions $f, g : \mathbb{C} \to \mathbb{C}$ we have $\mathcal{D}f(x) = g(x)$. To solve for f, we introduce a *Green's function*: $\mathcal{G}(x, x') : \mathbb{C}^2 \to \mathbb{C}$ such that $\mathcal{D}\mathcal{G}(x, x') = \delta(x - x')$. The particular solution of f then is[13]

$$f(x) = \int dx' \mathcal{G}(x, x') g(x') \tag{A.20}$$

One can easily check this by applying the differential operator on both sides.

$$\begin{aligned}
\mathcal{D}f(x) &= \mathcal{D} \int dx' \mathcal{G}(x, x') g(x') \\
&= \int dx' \mathcal{D}\mathcal{G}(x, x') g(x') \\
&= \int dx' \delta(x - x') g(x') \\
&= g(x)
\end{aligned}$$

Although these Green's functions construct the solutions to the differential equation, the proof is not constructive, i.e. we have not discussed an explicit procedure of calculating $\mathcal{G}$. Often, such a general construction method is not necessary.

A.3.2 Classical series expansion

Let us describe a classical particle travelling in time from t to t'. At any time $t_* \in (t, t')$ there is a chance $P(A)$ that some event A occurs, for example scattering at a fixed particle at position $\vec{R}$. This may happen at any time in the trajectory and it may happen more often than once. We are interested in the total probability that a particle starting at $\vec{r}$ ends at $\vec{r'}$. Let P_0 be the probability of any trajectory without scattering.

We will sum over all the different probabilities of A to obtain the total probability. We distinguish the outcomes where A happens once with the outcomes where A happens twice, etc. Thus,

$$\begin{aligned}
P(\vec{r}, t; \vec{r'}, t') &= P_0(\vec{r}, t; \vec{r'}, t') + \int dt_1 \; P_0(\vec{r}, t; \vec{R}, t_1) P(A) P_0(\vec{R}, t_1; \vec{r'}, t') \\
&+ \int \int dt_1 dt_2 \; P_0(\vec{r}, t; \vec{R}, t_1) P(A) P_0(\vec{R}, t_1; \vec{R}, t_2) P(A) P_0(\vec{R}, t_2; \vec{r'}, t') + \dots
\end{aligned} \tag{A.21}$$

Equation A.21 is a summation of all probabilities to get from $\vec{r}$ to $\vec{r'}$ in time $t' - t$. The integrals ensure that the scattering is allowed to happen at any $t_* \in (t, t')$. Since we are only interested in the time difference $t - t'$, we will write $P(\vec{r}, \vec{r'}, t - t') := P(\vec{r}, t; \vec{r}, t')$. Fourier transforming $P(\vec{r}, \vec{r'}, t - t')$ in the variable $t - t'$ will simplify equation *A*.21. Namely, if $P_0(\vec{r}_i, \vec{r}_j, t_i - t_j) = \frac{1}{2\pi} \int d\omega e^{-i\omega(t_i - t_j)} P_0(\vec{r}_i, \vec{r}_j, \omega)$, then

$$\begin{aligned}
&\int dt_1 \, P_0(\vec{r}, \vec{R}, t - t_1) P(A) P_0(\vec{R}, \vec{r'}, t_1 - t') \\
&\quad = \int dt_1 \Big\{ \frac{1}{2\pi} \int d\omega e^{-i\omega(t - t_1)} P_0(\vec{r}, \vec{R}, \omega) \Big\} P(A) \Big\{ \frac{1}{2\pi} \int d\omega' e^{-i\omega'(t_1 - t')} P_0(\vec{R}, \vec{r'}, \omega) \Big\} \\
&\quad = \frac{1}{(2\pi)^2} \int d\omega \int d\omega' P_0(\vec{r}, \vec{R}, \omega) P(A) P_0(\vec{R}, \vec{r'}, \omega') e^{+i(\omega' t' - \omega t)} \int dt_1 e^{-it_1(\omega' - \omega)} \\
&\quad = \frac{1}{(2\pi)^2} \int d\omega \int d\omega' P_0(\vec{r}, \vec{R}, \omega) P(A) P_0(\vec{R}, \vec{r'}, \omega') e^{+i(\omega' t' - \omega t)} \cdot 2\pi \delta(\omega' - \omega) \\
&\quad = \frac{1}{2\pi} \int d\omega e^{-i\omega(t - t')} P_0(\vec{r}, \vec{R}, \omega) P(A) P_0(\vec{R}, \vec{r'}, \omega')
\end{aligned} \tag{A.22}$$

This holds for all terms in the summation, hence we can write the summation in the Fourier domain without any integrals, equation A.23.

$$P(\vec{r}, \vec{r'}, \omega) = P_0(\vec{r}, \vec{r'}, \omega) + P(\vec{r}, \vec{r}_1, \omega) P(A) P_0(\vec{r}_1, \vec{r'}, \omega) + \dots \tag{A.23}$$

We will assume that the probability of one point in space to another with frequency ω without the occurance of event A is equal to some constant c. Equation A.23 can then be simplified to $P(\vec{r}, \vec{r'}, \omega) = c + cP(A)c + cP(A)cP(A)c + \cdots = c \cdot (1 + cP(A) + (cP(A))^2 + (cP(A))^3 + \dots) = c \cdot \frac{1}{1 - cP(A)}$, thus by this geometric series, we find

$$P(\vec{r}, \vec{r'}, \omega) = \frac{1}{c^{-1} - P(A)} \tag{A.24}$$

A.3.3 Greening of quantum mechanics

With A.20 we can rewrite the unperturbed Schrödinger equation, $\big[\frac{\nabla^2}{2m} + i\partial_t\big] \psi(\vec{r}, t) = 0$, as

$$\big[\frac{\nabla^2}{2m} + i\partial_t\big] G(\vec{r}, \vec{r'}; t, t') = \delta(\vec{r} - \vec{r'}) \delta(t - t') \tag{A.25}$$

By Fourier transforming (over the variable $\vec{r} - \vec{r'}$) we remove the spatial delta function: $\big[-\frac{k^2}{2m} + i\partial_t\big] G(\vec{k}; t, t') = \delta(t - t')$. The solution to this differential equa-

tion is[§]

$$G(\vec{k};t,t') = -i\theta(t-t')e^{-i\epsilon_k(t-t')} =: G_0 \tag{A.26}$$

This Green's function is called the free propagator. In the previous section we have seen a classical analogue of this function and we called its value c. All other propagators can be written in terms of G_0. To see this, we include a perturbation in the Schrödinger equation: $\left[\frac{\nabla^2}{2m} + i\partial_t - V(\nabla)\right]\psi(\vec{r},t) = 0$, which leads to the Green's function in $k-$space: $\left[-\frac{k^2}{2m} + i\partial_t - V(\vec{k})\right]G(\vec{k};t,t') = 0$. The solution is

$$G(\vec{k};t,t') = G_0(\vec{k};t,t') + \int dt'' G_0(\vec{k};t,t'')V(\vec{k})G(\vec{k};t'',t') \tag{A.27}$$

This can be seen by plugging equation A.27 into the perturbed Schrödinger equation. The solution should remind us of equation A.21: the last Green's function, $G(\vec{k};t'',t')$, may be expanded with the same formula. We have a recursive formula consisting of free propagators to calculate a propagator for the perturbed Hamiltonian. Once again, a Fourier transformation over $t-t'$ removes all the integrals. We are left with the *Dyson equation*, equation A.28.

$$G(\vec{k},\omega) = G_0(\vec{k},\omega) + G_0(\vec{k},\omega)V(\vec{k})G(\vec{k},\omega) \tag{A.28}$$

Analogous to the classical series expansion, we may utilise a geometric serie to solve for G[¶].

$$G(\vec{k},\omega) = \frac{G_0(\vec{k},\omega)}{1 - G_0(\vec{k},\omega)V(\vec{k})} = \frac{1}{G_0^{-1}(\vec{k},\omega) - V(\vec{k})} \tag{A.29}$$

The Fourier transformed free propagator is $G_0(\vec{k},\omega) = \frac{1}{\omega-\epsilon_k}$, therefore the total Green's function becomes

$$G(\vec{k},\omega) = \frac{1}{\omega - \epsilon_k - V(\vec{k})} \tag{A.30}$$

The function diverges at $\omega = \epsilon_k + V(\vec{k})$. This encompasses the power of Green's functions: the physical properties are present in equation A.30 - in particular, one can construct the DOS by isolating the imaginary part, so $\rho(\omega) = \mathfrak{Im}\, G(\omega - i\eta)$ for some small number η[6]. This fact will be used on the Anderson impurity model in section B.3.

Before applying the theory of Green's functions to this model, we will state the difference between the propagators from this section and the probabilities from section A.3.2. $P(\vec{k};t,t')$ is the probability that a particle travelling from time

[§]Here, ϵ_k is defined by $\hat{H}_0\phi_k = \epsilon_k\phi_k$ where $\hat{H}_0$ is the unperturbed single particle Hamiltonian and ϕ_k is the $k-$eigenstate.

[¶]Mathematically speaking we need $|GV| < 1$ for convergence, but it is customary in physics to assume that the analytical continuation to the divergent region is allowed.

t to time t' ends in the same state ϕ_k as the initial state. $G(\vec{k}; t, t')$, however, is the *probability amplitude*, which means that $P_0 = G_0^* G_0$. This does not imply $P = G^* G$, since $G^* G$ misses the interference terms of P.

Version of June 24, 2022– Created June 24, 2022 - 13:49

Appendix B

Anderson impurity model

A significant part of this appendix is based on the educational paper *'Local moment physics in heavy electron systems'* by P. Coleman[6].

B.1 Different terms in Hamiltonian

The objective of the Anderson impurity model is to describe the coupling between two separately solvable systems, a lattice and an impurity. The lattice solutions are electrons with a continuum of wavenumbers k and the impurity solutions are orbitals of maximally two electrons due to the Pauli exclusion principle. Not only the tunnelling is ought to be described, but also the possible Coulomb repulsion between two impurity electrons.

Let $\epsilon_{k\sigma}$ be the energy of a $|k\sigma\rangle$ electron in the lattice and E_d the energy of an electron in the impurity ($|d\sigma\rangle$). Let U be the extra energy term in the case of Coulomb repulsion between impurity electrons. Further, we will call $\mathcal{H}_{lat}$ the Hilbert space of the lattice and $\mathcal{H}_{imp}$ of the impurity. Let $\hat{c}^\dagger_{k\sigma}$, $\hat{c}_{k\sigma}$ be the creation and annihilation operator of lattice electrons and $\hat{d}^\dagger_\sigma$, $\hat{d}_\sigma$ of impurity electrons.

Let us assume that the lattice has n electrons with $\sigma =\uparrow$ and n electrons with $\sigma =\downarrow$. We choose the basis of $\mathcal{H}_{lat}$ to be $e_1 = |k_1 \uparrow\rangle, e_2 = |k_1 \downarrow\rangle, \ldots, e_{2n-1} = |k_n \uparrow\rangle$, $e_{2n} = |k_n \downarrow\rangle$ and the basis of $\mathcal{H}_{imp}$ to be $f_1 = |d \uparrow\rangle$, $f_2 = |d \downarrow\rangle$. This means that the Hamiltonian of $\mathcal{H}_{lat} \bigoplus \mathcal{H}_{imp}$ is

$$\hat{H} = \left[\begin{array}{ccccc|cc}
\epsilon_{k_1} & 0 & \ldots & & \varnothing & \langle k_1 \uparrow|\hat{H}|d \uparrow\rangle & 0 \\
0 & \epsilon_{k_1} & 0 & & & 0 & \langle k_1 \downarrow|\hat{H}|d \downarrow\rangle \\
\vdots & 0 & \ddots & 0 & \vdots & \vdots & \vdots \\
 & & 0 & \epsilon_{k_n} & 0 & \langle k_n \uparrow|\hat{H}|d \uparrow\rangle & 0 \\
\varnothing & & \ldots & 0 & \epsilon_{k_n} & 0 & \langle k_n \downarrow|\hat{H}|d \downarrow\rangle \\
\hline
\langle d \uparrow|\hat{H}|k_1 \uparrow\rangle & 0 & \ldots & \langle d \uparrow|\hat{H}|k_n \uparrow\rangle & 0 & E_d & \frac{U}{2} \\
0 & \langle d \downarrow|\hat{H}|k_1 \downarrow\rangle & \ldots & 0 & \langle d \uparrow|\hat{H}|k_n \uparrow\rangle & \frac{U}{2} & E_d
\end{array}\right]$$

The upper left block components of the diagonal make up $H_{lat}^{(0)}$ and the lower right block components of the diagonal make up $H_{imp}^{(0)}$. The lower right block off-diagonal components account for the Coulomb repulsion. The unknown matrix elements are in the upper right and lower left block and belong to the perturbation. Let us call $V_k = \langle k\sigma|\hat{H}'|d\sigma\rangle$ the hybridisation energy. Hereby, we assume that this energy is independent of the spins of the electrons.

From the matrix representation of the Hamiltonian, we deduce the second quantised form, equation B.1.

$$\hat{H} = \sum_{k\sigma} \epsilon_{k\sigma}\hat{n}_{k\sigma} + \sum_{\sigma} E_d\hat{n}_{d\sigma} + U\hat{n}_{d\uparrow}\hat{n}_{d\downarrow} + \sum_{k\sigma} V_k\hat{c}_{k\sigma}^{\dagger}\hat{d}_{\sigma} + H.C. \tag{B.1}$$

Here, $\hat{n}_{k\sigma}$ denotes $\hat{c}_{k\sigma}^{\dagger}\hat{c}_{k\sigma}$ and $\hat{n}_{d\sigma}$ denotes $\hat{d}_{\sigma}^{\dagger}\hat{d}_{\sigma}$. Only the last term, $\sum_{k\sigma} V_k\hat{c}_{k\sigma}^{\dagger}\hat{d}_{\sigma} + H.C.$, is a perturbation - the rest of the Hamiltonian can be analytically solved.

B.2 Perturbative expansion

We will construct equivalent interactions to the Hartree approximation to obtain the Green's function of an impurity electron, $|d\sigma\rangle$. The term, $V(\vec{k})$, in equation A.30 is $U\langle\hat{n}_{d\overline{\sigma}}\rangle$ for the Coulomb repulsion such that $\overline{\sigma}$ is the opposite spin of σ. Namely, $V(\vec{k}) = U\langle\hat{n}_{d\uparrow}\rangle\langle\hat{n}_{d\downarrow}\rangle$, but $\langle\hat{n}_{d\sigma}\rangle = 1$ is already given, since we describe its propagator.

Finding the term, $V(\vec{k})$, for the second interaction type requires a few more steps. We notice that, in order for the electron to interact with the lattice and ending as an impurity electron, it needs to undergo at least two interactions: coupling to the lattice and coupling back to the impurity. Suppose, the first has an amplitude of V_k and the second of V_k^*. Between these successive events, there is a free lattice propagator, $G_0(\vec{k},\omega) = \frac{1}{\omega-\epsilon_k}$. Since, there are more values of k, we need to sum over all k. By multiplying the individual events, we obtain $V(\vec{k}) = \sum_k \frac{|V_k|^2}{\omega-\epsilon_k}$. The result of the geometric series is

$$G_{d\sigma}(\omega) = \frac{1}{\omega - E_d - \sum_k \frac{|V_k|^2}{\omega-\epsilon_k} - U\langle\hat{n}_{d\overline{\sigma}}\rangle} \tag{B.2}$$

B.3 Density of states

Suppose the impurity DOS is sharply peaked around some energy ϵ. By coupling the impurity to the lattice, the DOS will broaden. Quantitatively, the uncertainty in energy of an impurity electron due to the hybridisation to the lattice can be calculated by Fermi's golden rule, $\Delta E = \pi\sum_k |V_k|^2\delta(\epsilon_k - \epsilon)$. Let us define the function, $\Sigma(\omega) := \sum_k \frac{|V_k|^2}{\omega-\epsilon_k}$ for convenience. Then,

Version of June 24, 2022– Created June 24, 2022 - 13:49

$$\begin{aligned}\Sigma(\omega - i\eta) &= \sum_k \frac{|V_k|^2}{\omega - \epsilon_k - i\eta} \\ &= \int d\epsilon \sum_k \frac{|V_k|^2}{\omega - \epsilon - i\eta}\delta(\epsilon - \epsilon_k) \\ &= \frac{1}{\pi}\int d\epsilon \frac{1}{\omega - \epsilon - i\eta}\pi \sum_k |V_k|^2 \delta(\epsilon - \epsilon_k) \\ &= \frac{1}{\pi}\int d\epsilon \frac{\Delta E}{\omega - \epsilon - i\eta} \\ &= -\frac{1}{\pi}\int d(\omega - \epsilon)\frac{\Delta E}{\omega - \epsilon - i\eta}\end{aligned} \tag{B.3}$$

We will assume that the uncertainty, ΔE, remains approximately constant over the integration region $(-D, D)$; $\Delta := \Delta E$, and we will choose D such that $\omega \ll D$. We will omit terms of order $\mathcal{O}(\frac{\omega}{D})$. By the Sokhotski-Plemelj theorem, we find that

$$\begin{aligned}\Sigma(\omega - i\eta) &= -\frac{1}{\pi}\Big[i\pi\Delta + \mathcal{P}\int d(\omega - \epsilon)\frac{\Delta}{\omega - \epsilon}\Big] \\ &= -i\Delta - \frac{\Delta}{\pi} ln|\frac{\omega - D}{\omega + D}| = -i\Delta - \frac{\Delta}{\pi} ln(\frac{D - \omega}{D + \omega}) \\ &= -i\Delta - \frac{\Delta}{\pi} ln(1 - 2\frac{\omega}{D + \omega}) \approx -i\Delta - \frac{\Delta}{\pi} ln(1 - 2\frac{\omega}{D}) \\ &\approx -i\Delta - 2\frac{\omega}{D} - 2(\frac{\omega}{D})^2 - \frac{8}{3}(\frac{\omega}{D})^3 - 4(\frac{\omega}{D})^4 \approx -i\Delta\end{aligned} \tag{B.4}$$

Therefore, $G_{d\sigma}(\omega - i\eta) = \frac{1}{\omega - (E_d + U\langle n_{d\bar{\sigma}}\rangle) - i\Delta}$. We can now construct the DOS by taking the imaginary part of this Green's function.

$$\begin{aligned}\rho_{d\sigma}(\omega) &= \frac{1}{\pi}\mathfrak{Im} G_{d\sigma}(\omega - i\eta) \\ &= \frac{1}{\pi}\mathfrak{Im}\frac{1}{\omega - (E_d + U\langle n_{d\bar{\sigma}}\rangle) - i\Delta} \\ &= \frac{1}{\pi}\mathfrak{Im}\frac{\omega - (E_d + U\langle n_{d\bar{\sigma}}\rangle) + i\Delta}{\Big(\omega - (E_d + U\langle n_{d\bar{\sigma}}\rangle)\Big)^2 + \Delta^2} \\ &= \frac{1}{\pi}\frac{\Delta}{\Big(\omega - (E_d + U\langle n_{d\bar{\sigma}}\rangle)\Big)^2 + \Delta^2}\end{aligned} \tag{B.5}$$

This function is called a *Lorentz distribution*.

Bibliography

[1] G. Rajasekaran, arXiv:1606.08715.

[2] A. Taroni, Nobel Prize 2015: Kajita and McDonald. Nature Phys 11, 891 (2015).

[3] Y. Cheipesh, V. Cheianov, A. Boyarsky, Phys. Rev. D 104, 116004 (2021).

[4] V. Brdar, R. Plestid, N. Rocco, Phys. Rev. C 105, 045501 (2022).

[5] Y. Hochberg, Y. Kahn, M. Lisanti, C.G. Tully, K.M. Zurek arXiv:1606.08849.

[6] P. Coleman, arXiv:cond-mat/0206003.

[7] M. Pivetta, S. Rusponi, H. Brune, Phys. Rev. B 98, 115417 (2018).

[8] A.H. Castro Neto, F. Guinea, N.M.R. Peres, K.S. Novoselov, A.K. Geim Rev. Mod. Phys. 81, 109 (2009).

[9] A.L. Kozub, A.B. Shick, F. Máca, J. Kolorenč, A.I. Lichtenstein, Phys. Rev. B 94, 125113 (2016).

[10] N. Aghanim et al. (Planck Collaboration), arXiv:1807.06209.

[11] A. Altland, B.D. Simons (Cambridge, 2010, second edition), Condensed Matter Field Theory, Cambridge University Press.

[12] R.D. Mattuck (Dover, 1992, second edition), A Guide to Feynman Diagrams in the Many-Body Problem, Dover Publications.

[13] M.M. Odashima, B.G. Prado, E. Vernek, Rev. Bras. Ens. Fis., 39, e1303 (2017).